Available online at BCREC website: https://bcrec.id

Bulletin of Chemical Reaction Engineering & Catalysis, 14 (3) 2019, 502-512

Research Article

Direct Synthesis of Sodalite from Indonesian Kaolin for Adsorption of Pb^{2+} Solution, Kinetics, and Isotherm Approach

Tri Wahyuni[1], Didik Prasetyoko[1*], S. Suprapto[1], Imroatul Qoniah[1], Hasliza Bahruji[2], Ahmad Dawam[1], Sugeng Triwahyono[3], Aishah Abdul Jalil[3]

[1]Department of Chemistry, Faculty of Science, Institut Teknologi Sepuluh Nopember, Keputih, Sukolilo, Surabaya 60111, Indonesia
[2]Centre of Advanced Material and Energy Sciences, Universiti Brunei Darussalam, Brunei Darussalam
[3]Ibnu Sina Institute for Fundamental Science Studies, Universiti Teknologi Malaysia, Skudai, Johor Bahru 81310, Malaysia

Received: 17th July 2018; Revised: 21st March 2019; Accepted: 23rd March 2019; Available online: 30th September 2019; Published regularly: December 2019

Abstract

Indonesian kaolin was used as precursor for synthesis of sodalite. Synthesis parameters were optimized by varying the Si/Al ratios, stirring and aging conditions, and water composition. X-ray diffraction (XRD), Fourier Transform Infra Red (FTIR), Scanning Electron Microscope-Energy Dispersive X-ray (SEM-EDX), and Particle Size Analyzer (PSA) were used to characterize sodalite. The potential of sodalite as adsorbent for heavy metal Pb^{2+} ions removal from waste water was investigated in this work. The uptake adsorption capacities of sodalite was 90-100 mg/g from synthesized sodalite crystallized for 24 and 48 hours, and commercial silica. The kinetic of Pb^{2+} adsorption was a pseudo second order reaction and the adsorption coefficients was followed Langmuir adsorption isotherm. Copyright © 2019 BCREC Group. All rights reserved

Keywords: Sodalite; Kaolin; kinetics; Pb^{2+} adsorption; Isotherm

How to Cite: Wahyuni, T., Prasetyoko, D., Suprapto, S., Qoniah, I., Bahruji, H., Dawam, A., Triwahyono, S., Jalil, A.A. (2019). Direct Synthesis of Sodalite from Indonesian Kaolin for Adsorption of Pb^{2+} Solution, Kinetics, and Isotherm Approach. *Bulletin of Chemical Reaction Engineering & Catalysis*, 14(3): 502-512 (doi:10.9767/bcrec.14.3.2939.502-512)

Permalink/DOI: https://doi.org/10.9767/bcrec.14.3.2939.502-512

1. Introduction

Industrial wastewater containing harmful heavy metals is a major threat causing serious health problem to the ecosystems. Lead is a non-biodegradable, hazardous heavy metal that accumulated and have adverse effect on human health. Studies showed lead affects caused serious damage to nervous system, kidney function and reproduction organ [1]. It also affects hematopoietic, renal, gastrointestinal, and cardiovascular [2]. Removal of lead from waste water using reverse osmosis, precipitation, ion exchange and electro dialysis have been investigated and were proven effective [1,3-6]. However, the processes were economically demanding and the waste deposit resulted from the removal processes were still required for additional disposal treatment.

Sorption using solid adsorbents offers a better solution for waste water treatment which in-

* Corresponding Author.
E-mail: didikp@chem.its.ac.id;
didik.prasetyoko@gmail.com (D. Prasetyoko);
Tel/fax: 62-31-5943353/62-31-5928314

cludes adsorption and precipitation reactions [3]. Hydroxyapatite [7], activated carbon [8], zeolite [9] have been used for heavy metal waste water treatment. Zeolites and polymer resins showed improved adsorption of heavy metal in large scale but activated carbon has lower adsorption capacity [10]. Zeolite is economically available which allowed the process to be carried out in large scale [11]. Studies on new adsorbents derived from low cost materials have attracted significant interests. Sodalite is a type of zeolites and has framework structure which consists of 6 rings and a pore size of 2.8 Å [12]. Sodalite has a great potential as heavy metal adsorbent due to its small pore size and high capacities for ion adsorption. Sodalite can be synthesized using abundantly occurring minerals for low cost production such as coal fly ash, rice hush ash and clay minerals [10,13,14]. Palygorskite clay materials produced sodalite with micro and submicro sized crystal [12]. Hydroxyl sodalite in the shape of corals was synthesized from rice husk ash as a source of silica [13]. Synthesis sodalite from rice hush ash without organic template resulting sodalite with nanocrystal size [15]. Sodalite was also synthesized from kaolinite which required treatment with NaOH prior to synthesis in order to activate kaolinite into metakaolin [16].

Adsorption of metal on alternative low cost material has attracted large interest to search for material with high adsorption capacities. In the previous study, mesoporous aluminosilicates have been prepared from Indonesian kaolinite clay without calcination [17]. Here, untreated Indonesian kaolinite was used as precursor for sodalite formation. The synthesis parameters including the SiO/Al_2O_3 ratios, the influence of stirring and aging treatment and also water content were investigated in detail in order to find the optimized conditions for synthesizing sodalite. The resulting products were used as adsorbent for Pb^{2+} metal removal from waste water.

2. Material and Methods

2.1 Materials

Sodalite was synthesized from kaolin (kaolinite, $Al_4(Si_4O_{10})(OH)_8$) obtained from Bangka Belitung, Indonesia, with the composition (wt%) Al_2O_3 (22%), SiO_2 (57%), P_2O_5 (3.9%), K_2O (3.22%), CaO (1.8%), TiO_2 (2.2%), V_2O_5 (0.15%), Fe_2O_3 (8.89%), CuO (0.31%), Ga_2O_3 (0.074%), ZrO_2(0.22%), and BaO (0.77%); NaOH (sodium hydroxide, pellets, Applichem, >99,5%); sodium aluminate anhydrous ($NaAlO_2$, sigma Aldrich, Al_2O_3 50-56%, Na_2O 40-45%) used as a source of alumina; demineralized water, stock solution of Pb^{2+} ion with concentration at 1000 ppm was prepared by dissolving $Pb(NO_3)_2$ solids (Merck) in distilled water.

2.2 Synthesis

The synthesis of sodalite was carried out by mixing 3 grams of kaolin and NaOH solution (2.2 grams of NaOH added into 26.4 grams of demineralized water) in a polypropylene bottle. The mixture was stirred for 15 minutes. Sodium aluminate (0.9 g) was then added into the mixture and stirred for another 15 minutes. The end product composition ratio is 3 Na_2O : 2 SiO_2 : 1 Al_2O_3 : x H_2O, where x is water composition, which is varied from 30, 60, 90, 128 and 200 (6.2; 12.4; 18.5; 26.4; 41.2 g). The mixture formed was stirred for 24 hours at room temperature. The gel formed was left to age at room temperature before placed in the oven at 100 °C, both for 24 hours. Afterwards, the mixture was cooled and filtered, and the solids were washed with demineralized water until it reached pH 9. The resulting sample was dried at 100 °C for 24 hours.

The composition ratio of sodalite synthesis was 3 Na_2O : 2 SiO_2 : 1 Al_2O_3 : 128 H_2O. The reaction mixtures was stirred at various time i.e. 1, 3, 6, 12, and 24 hours and aged for 24, 48 and 72 hours. The Si/Al ratio was also varied from 1.5 to 3.5 by changing the sodium aluminate composition.

2.3 Characterization

X-ray diffraction analysis was performed using Phillips Expert with Cu-Kα (40 kV, 30mA) radiations at a range between $2\theta = 5$ to 50^o. The infrared spectra (at a range of 400 to 1400 cm^{-1}) were used to find the molecule vibrations determined by using the FTIR (Shimadzu Instrument Spectrum One 8400S). SEM and EDX were analyzed using the ZEISS EVO MA 10 instrument for SEM and BRUKER 129 EV for EDX. The particle sizes were characterized by using the PSA (*particle size analyzer*) made by Malvern type zetasizer Ver. 7.01.

2.4 Determining the Adsorption

The ability of sodalite as adsorbent was determined using Pb^{2+} solution. The adsorption of Pb^{2+} was carried out by mixing of 0.05 grams of sodalite with a 200 mL (50 ppm) of $Pb(NO_3)_2$ solution. The mixture was stirred for 24 hours at room temperature. 10 mL of liquid sample was taken and filtered at the intervals of 20,

Copyright © 2019, BCREC, ISSN 1978-2993

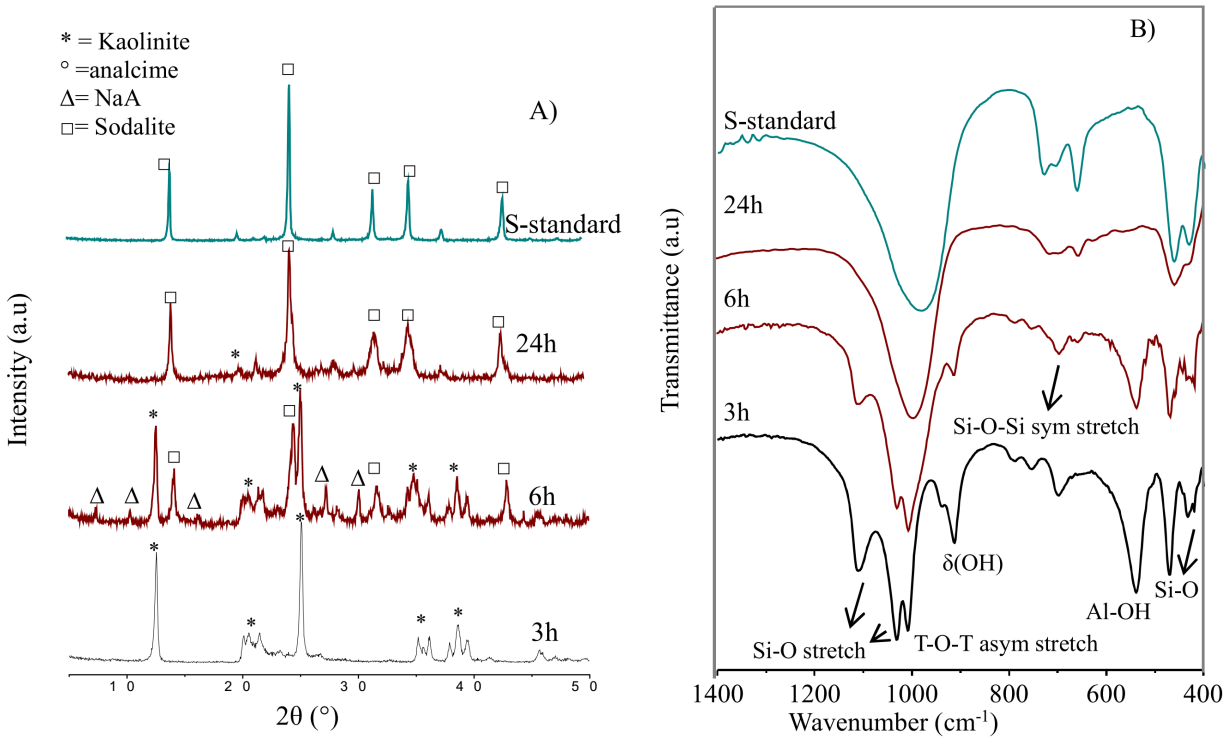

Figure 1. XRD diffractogram and infrared analysis data of the resulting solids obtained at 3 h, 6 h, 24 h period and sodalite synthesized from commercial silica (S-standard).

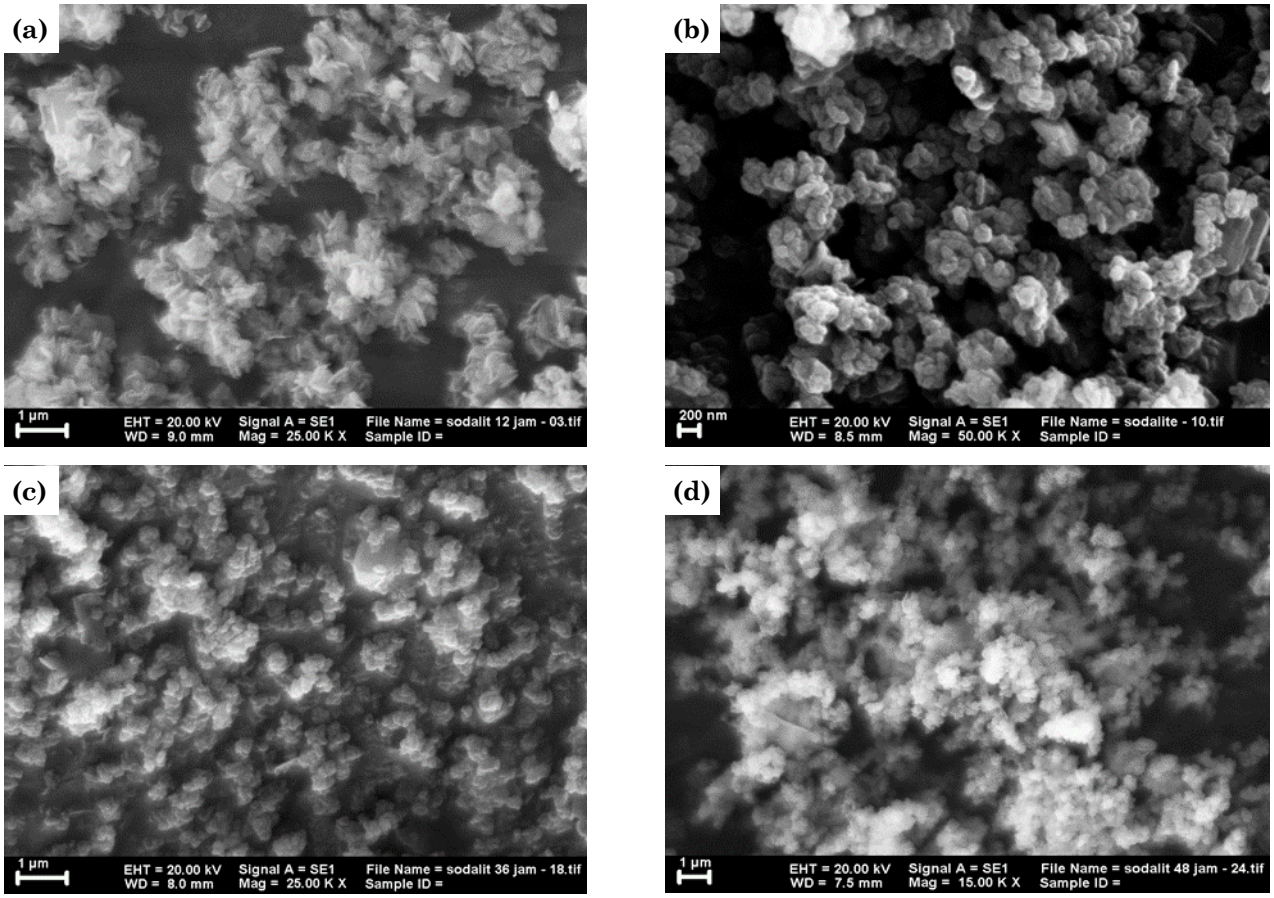

Figure 2. SEM images of synthesized powders at (a) 12, (b) 24, (c) 36, (d) 48 h of crystallization time

Copyright © 2019, BCREC, ISSN 1978-2993

30, 50, 80, 120, 170, 230, 300, 480, 720, and 1440 minutes to allow investigation towards the effect of contact time between sodalite and Pb^{2+} ion. The Pb^{2+} concentration was determined by using AAS (AA-6800, SHIMADZU) where the adsorption capacities were determined by using Equation (1). Meanwhile, the adsorption percentage was determined by using Equation (2).

$$q_e = \frac{(C_0 - C_e)V}{m} \quad (1)$$

$$R(\%) = \frac{C_0 - C_e}{C_0} \times 100 \quad (2)$$

Where, C_0 and C_e (mg.L^{-1}) are the concentration of Pb^{2+} solution initially and after the process of adsorption, respectively, V (liter) is the volume of Pb^{2+} solution, and m (grams) is the adsorbent (sodalite) mass that was used.

3. Results and Discussion

3.1 Sodalite formation from Indonesian kaolin

XRD diffraction and infrared spectroscopy were used to investigate the transformation of kaolin to sodalite. Kaolin is naturally occurring clay riches mineral with aluminum and silica that is suitable precursor for sodalite synthesis. The XRD analysis of kaolin clay in Figure 1(A) shows the peaks corresponded to kaolinite at 2θ = 12.3 and 24.8° [18].

XRD analysis of the synthesized products at various crystallization times are shown in Figure 1(B). As we increase the crystallization time, kaolinite phase was changed into zeolite NaA as evidence by the peak appeared at 2θ = 7.14° during the 3 h into treatment. Sodalite framework began to appear at 2θ = 14° on the solid product obtained after 6 hours of crystallization time [19]. We observed a pure sodalite crystalline framework with no traces of kaolinite and NaA phase after 24 h. The crystallinity however continued to improve as the synthesis were carried out for up to 48 h.

Infrared spectroscopy analysis provides information on the vibrational properties of aluminosilicate framework. The infrared spectra of the synthesized products are shown in Figure 1(B). The product obtained after 3 h of crystallization showed the crystalline phase was still dominated by kaolinite. The kaolinite

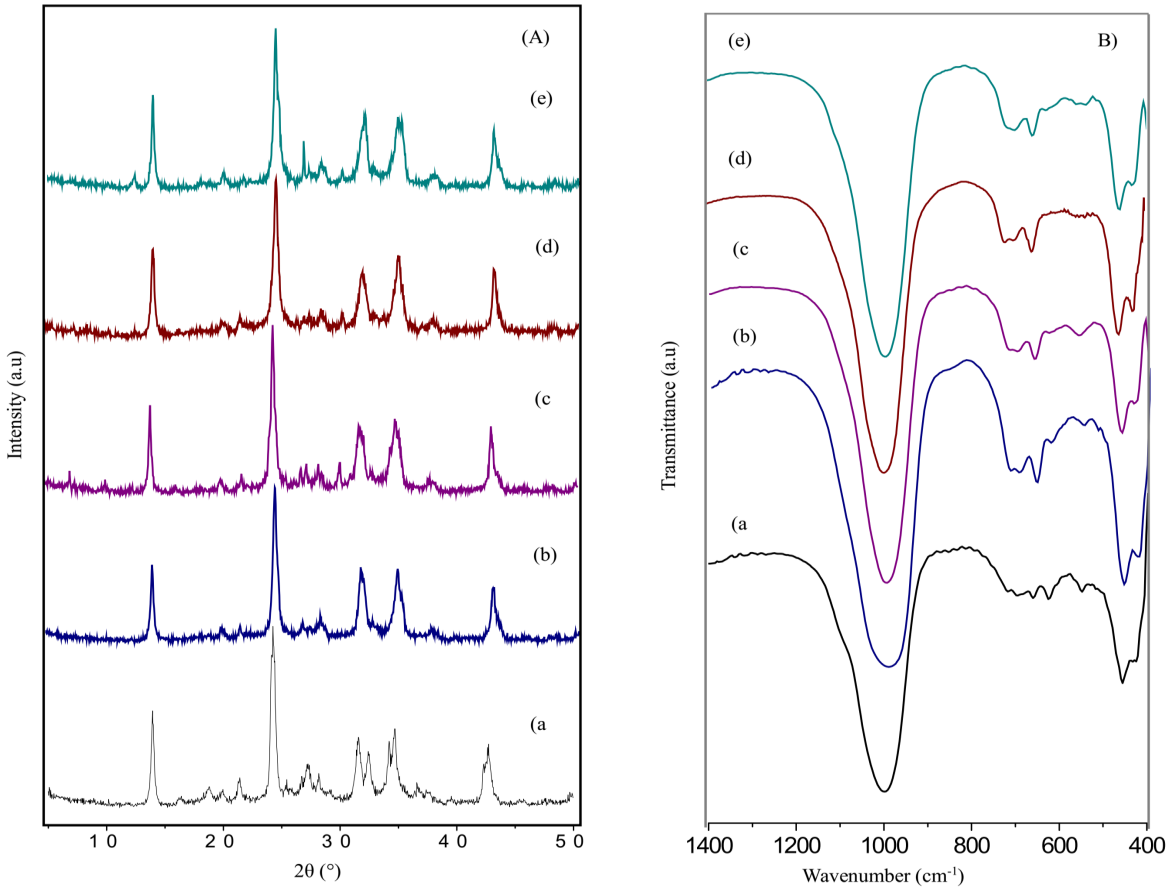

Figure 3. (A) XRD Patterns, (B) FT-IR Spectra for sodalite H_2O molar ratio of : (a) 30, (b) 60, (c) 90, (d) 128, (e) 200

Copyright © 2019, BCREC, ISSN 1978-2993

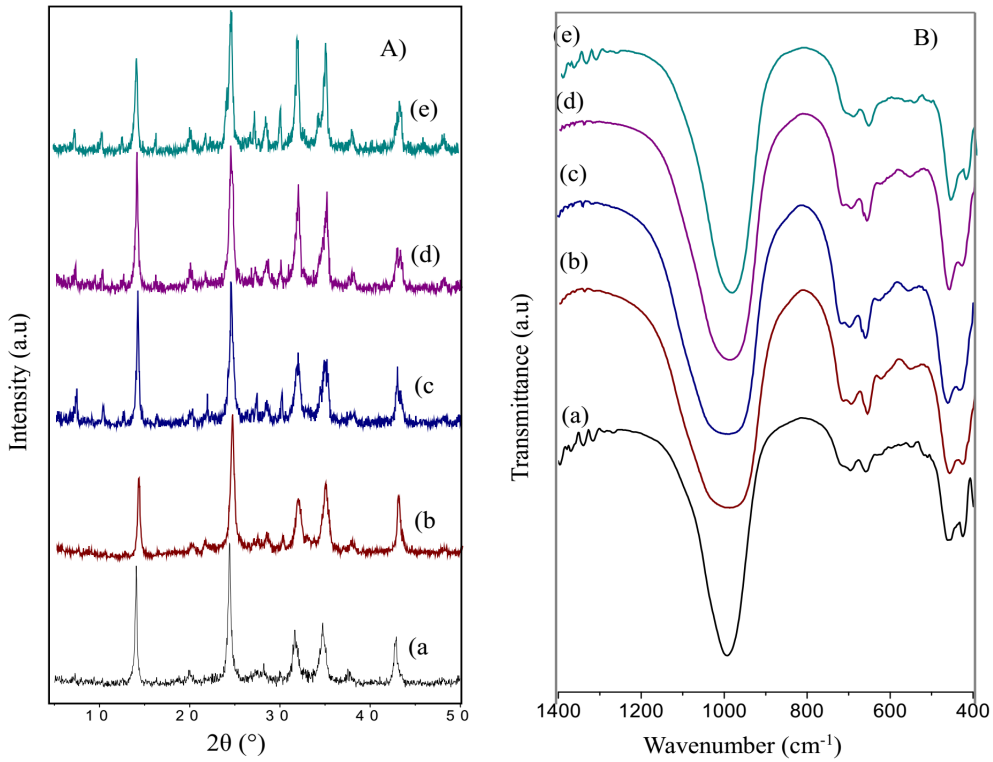

Figure 4. (A) XRD pattern, (B) FT-IR spectra for sodalite with SiO_2/Al_2O_3 molar ratio variations of (a) 1.5, (b) 2, (c) 2.5, (d) 3, (e) 3.5

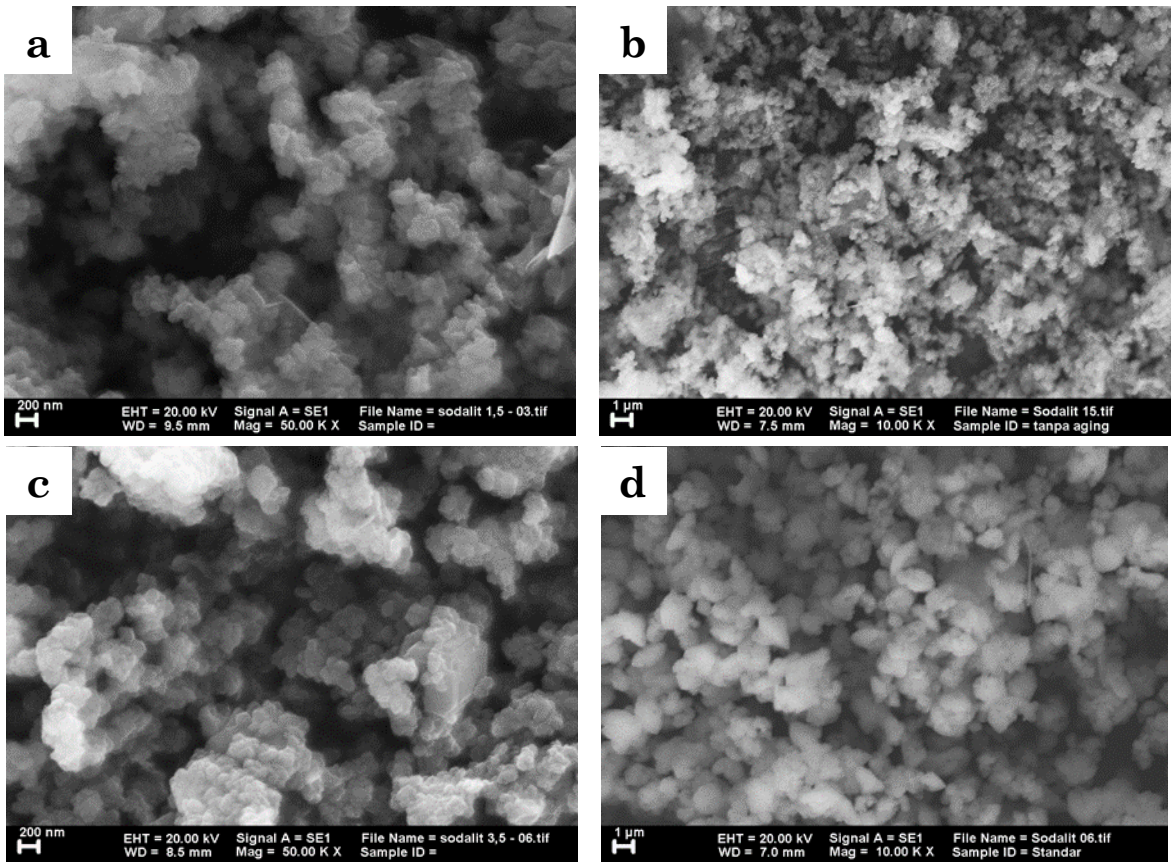

Figure 5. The morphology of synthesis results based on SEM characterization on the SiO_2/Al_2O_3 molar ratio variations of (a) 1.5, (b) 2, (c) 3.5, and (d) standard sodalite

Copyright © 2019, BCREC, ISSN 1978-2993

characteristic was confirmed by adsorption bands at 1030 and 1108 cm^{-1}, corresponded to Si–O stretching; 916 cm^{-1} for δ(OH); 756 and 789 cm^{-1} for Si–O–Si symmetric stretching; and 428 and 469 cm^{-1} for Si–O [18]. The dissolution process of kaolinite can be observed by Al–O and Al–OH deformation band at 696 cm^{-1} and 540 cm^{-1} which completely dissolved after 24 h. As the kaolinite structure disintegrated, the zeolite A framework started to form which shown by the disappearance of peak at 1030 cm^{-1}. A broad signal centered at 1008 cm^{-1} appeared which is corresponded to the T–O (T = Si or Al) asymmetric stretching. The T–O–T (T = Si, Al) vibrational peak at 990 cm^{-1} also shifted towards lower wavenumber suggested the increased of Al content into the T–O framework. Sodalite was formed at 24 h of crystallization evident by peaks indicated to T–O–T symmetrical stretched appeared at 734, 707 and 663 cm^{-1} [15]. At wavelength 438 cm^{-1}, the samples showed an O–T–O bending vibration, whilst single 4 rings (S4R) was observed at wavelength 430 cm^{-1} [13].

The SEM images of the synthesized products at crystallization time of 12, 24, 36, and 48 h are shown in Figure 2. For sample obtained at 12 h, XRD confirmed the crystalline phase was mainly kaolinite with particle size of 1 μm. The morphology of the crystals showed a mixture of rod like structures and cubical aggregates. The crystallite size was reduced to 200 nm at 24 h of crystallization. The rod like morphology was disappeared with new form of spherical aggregates appeared. The crystallite maintained the sphere morphology with the crystal growth into 1 μm after 36 and 48 h. Meanwhile, we also use Particle Size Analyzer to determine crystal size of synthesized sodalite. For sample obtained after 24 hours of crystallization, the particle sizes were ~ 170 to 585 nm, may be due no aggregation of the particle.

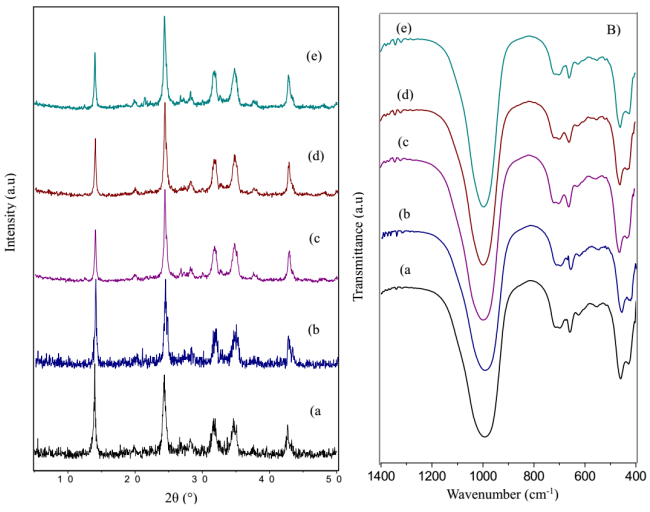

Figure 6. (A) XRD Pattern, (B) FT-IR Spectra to predict synthesis products based on stirring time variations of (a) 1, (b) 3, (c) 6, (d) 12, (e) 24 hours

3.2 The influence of water composition and SiO_2/Al_2O_3 ratios on sodalite formation

Water plays important role in hydrothermal synthesis of zeolite [20]. By controlling water composition from 30, 60, 90, 120 and 200 in the initial reaction mixtures, it will be able to provide an insight into its effect on dissolution of kaolin and formation of sodalite. The XRD pattern (Figure 3(A)) showed that pure phase of sodalite were only obtained when water composition was more than 60. Kaolinite phase evident by peaks at 2θ = 31 dan 34° was still visible when water ratio was fixed at 30. Increasing water composition while the amount of NaOH ratios were constant, the percentage of sodalite crystal obtained were significantly reduced (Table 1) which suggested the dissolving rate of kaolinite was affected at low alkalinity of the solution. XRD analysis was also supported by infrared analysis that revealed the presence of kaolinite for product obtained when water composition was at 30 (Figure 3(B)). Adsorption band appeared at 694 cm^{-1} corresponded to the deformation of AlO–H further proved that water was important to accelerate the dissolution of kaolinite [18]. For products obtained at water composition of 60 to 200, sodalite characteristics appeared evident by single 4 rings vibrations at 432 and 432 cm^{-1} together with asymmetrical strain and symmetrical strain of T–O–T (T = Si, Al) at 995 cm^{-1} and 700 and 659 cm^{-1} [13].

Tabel 1. Effects of H_2O composition and Si/Al ratio ratio towards crystallinity and particle size

Parameters	Water composition					Si/Al ratio				
	30	60	90	128	200	1.5	2	2.5	3	3.5
Crystallinity, %	22.4	28.8	27.7	22.2	22.3	9.8	22.2	7.6	7.7	3.7
Particle size, nm	36	35.9	39	35.5	38.1	40.8	35.5	38	35.8	33.8

Copyright © 2019, BCREC, ISSN 1978-2993

The effect SiO_2/Al_2O_3 ratios on sodalite formation was investigated by varying the composition of sodium aluminate. The initial SiO_2/Al_2O_3 ratio was maintained at 3 and sodium aluminate was added to reduce the ratios to 1.5, 2.0, 2.5, and 3.0. XRD analysis of the resulting products illustrated in Figure 4(A) showed the presence of sodalite evident by peaks at 2θ =14°. However, only samples with SiO_2/Al_2O_3 ratios of 1.5 and 2 showed only sodalite crystalline phase. As for SiO_2/Al_2O_3 molar ratios of 2.5, 3 and 3.5, the presence of zeolite A was clearly visible by a peak appeared at 2θ = 7.14°. This is also supported by infrared analysis (Figure 4(B)) which shown the adsorption band at 555 cm^{-1} corresponded to the double 4 rings (D4R) adsorption from zeolite A [21]. The crystallinity of the synthesized sodalite was calculated based on the diffraction peak at 29° as relative to the standard sodalite.

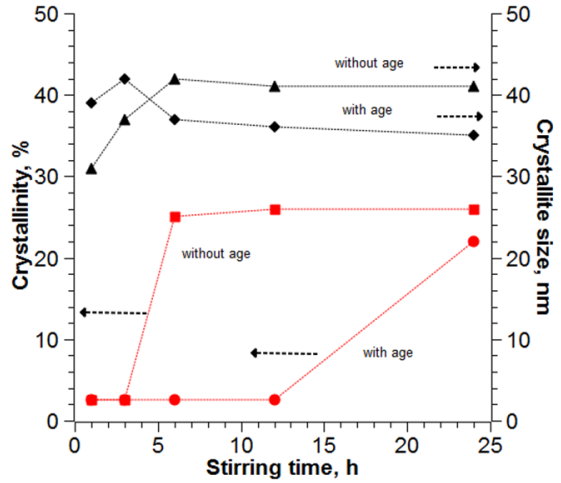

Figure 7. The influence of stirring and aging on the size of crystallite and crystallinity of sodalite

The sodalite showed significant decreased in crystallinity at higher SiO_2/Al_2O_3 ratios.

Figure 5 showed the morphology of the synthesized sodalite obtained from SEM. The submicron sodalite crystals were formed on the SiO_2/Al_2O_3 ratios of 1.5; 2; 3.5 and standard sodalite. The crystallite sizes of sodalite is 200 nm (Table 1) on the SiO_2/Al_2O_3 molar ratio of 2. On the same SiO_2/Al_2O_3 molar ratio, there are also the sodalite synthesized by commercial silica particle sizes of 1 μm and morphology being observed that took the form of aggregates with sizes of approximately 200 nm. The SiO_2/Al_2O_3 molar ratio has a crucial role in forming the morphology and particles sizes of sodalite [12].

3.3 The influence of stirring and aging on the transformation of kaolin to sodalite

In order to optimize the parameter affecting sodalite synthesis from kaolin clay minerals, we varied the stirring time and allowed the reaction mixture to age. Aging was defined as time allocated in between the process of mixing reactants and hydrothermal process. Table 2 summarized the physical properties of synthesized sodalite and Figure 7 illustrated the changes on crystallinity and crystal size with varied stirring and aging processes. The XRD and infrared analysis (Figure 8) showed that sodalite was formed from all reaction mixture. Figure 7 showed that the product crystallinity were improved with prolonged stirring to give 25% after 5 h of stirring. Further stirring up to 24 h shows negligible improvement on the crystallinity of the as-synthesized sodalite. Aging was reported to have positive impacts on the nucleation process and the growth of zeolite crystal [22]. It is interesting to see aging has no significant improvement on the crystallinity of sodalite and its crystallite size. The percent-

Table 2. Crystalline phase, crystallinity and crystallite size of samples obtained with varied stirring and aging time

Stir, h	Crystalline phase	Without aging		24 h aging	
		Crystallinity, %	Size, nm	Crystallinity, %	Size, nm
1	K, S	2.5	32	2.5	39
3	K,S,A	2.3	39	2.7	42
5	S,A	25	42	2.8	37.5
12	S,A	25	41	3	36.5
24	S,A	25	40	23	36.5
				[a]25	[a]41
				[b]24	[b]37

[a] sample was left to age for 48 h
[b] aged for 72 h
K – kaolinite, S- sodalite, A-amorphous

Copyright © 2019, BCREC, ISSN 1978-2993

age of sodalite crystallinity phases were significantly affected, to give only ~ 2% from reaction mixtures that were subjected to stirring and aging processes. Crystallinity has been estimated for the synthesized samples by taking sum of relative intensities of ten individual characteristic peaks [25] (Equation (3)).

$$\frac{Sum\ total\ of\ relative\ intensity\ of\ zeolite}{Sum\ total\ of\ relative\ intensity\ of\ standard} \times 100 \qquad (3)$$

Figure 7 also revealed the effect of stirring and aging on the size of sodalite crystal obtained from the reaction. The crystal sizes determined form XRD peaks were around 40 nm for all samples. Although the crystal size only showed slight differences between aging and stirring, we can observed trend that suggested that leave the mixture to age before hydrothermal treatment produced smaller crystal. It is important to note that prolonging the aging treatment for to 48 h and 72 h on the mixture that was stirred for 24 h have no significant improvement on the crystallinity and the crystallite size of sodalite.

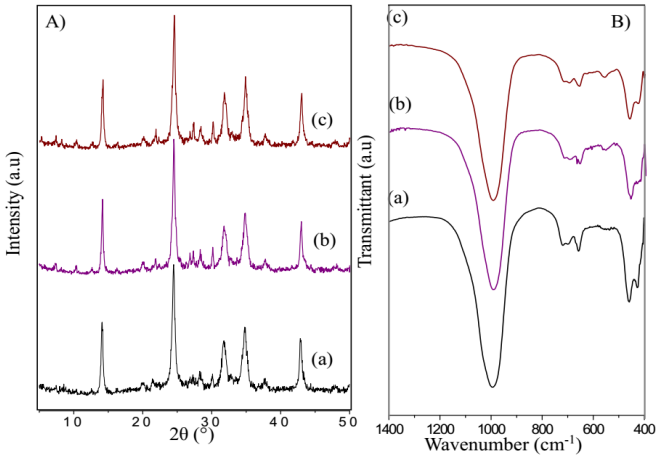

Figure 8. (A) XRD pattern and (B)FT-IR spectra based on effects of aging time (a) 24, (b) 48, (c) 72 hours.

3.4 Pb^{2+} Adsorption Using Sodalite

3.4.1 Effects of contact time

The ability of sodalite as adsorbent was determined on the adsorption of ion Pb^{2+}. Two sodalite samples with SiO_2/Al_2O_3 ratio of 2 that were synthesized for 24 and 48 h were used for the reaction and the samples were labelled as S-24 and S-48. The Pb^{2+} adsorption uptake of the synthesized sodalite was also compared to sodalite obtained from commercial silica (labelled as S-standard), sodalite pallets and activated carbon. The plot of Pb^{2+} adsorption against varied contact times between 20 to 1440 mins was shown in Figure 9. Rapid adsorption of heavy metals (Pb^{2+}) was observed 20 mins into the reaction and the adsorption continued to increase to reach steady state at 720 mins. Rapid adsorption at the beginning of the reaction suggested the formation of strong interaction between Pb^{2+} and the vacancy sites on the sodalite surface [20]. The adsorption capacity (Qe) was determined based on the adsorption at 720 mins when the value reached steady state. The Qe value for the S-24; S-48; and S-standard samples are comparable at ~ 95 - 100 mg/g. These results are higher when in comparison to the adsorption capacity (Qe) of the sodalite pellets and activated carbons, ~ 10 mg/g [16].

3.4.2 Kinetic adsorption approach

Kinetic adsorption approach was used to determine the order of Pb^{2+} adsorption into the sodalite surface. The Pb^{2+} kinetic adsorption was determined using the pseudo first and sec-

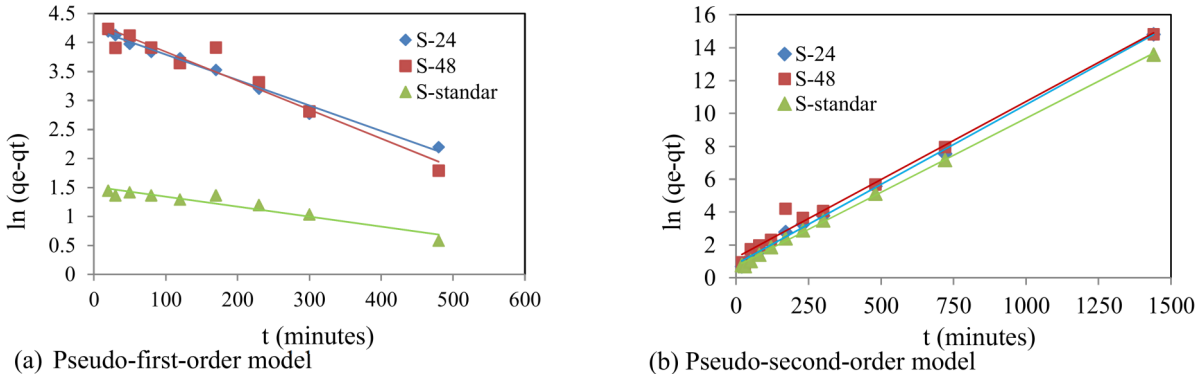

Figure 9. Graphs showing the Pb^{2+} kinetic adsorption by sodalite with different samples; S-24, S-48 (crystallization time of 24 and 48 hours) and S-standard (standard sodalite)

Copyright © 2019, BCREC, ISSN 1978-2993

ond order equations given as follows:

$$ln(q_e - q_t) = ln\, q_e - k_1 t \quad (3)$$

$$\frac{t}{q_t} = \frac{1}{k_2 q_e^2} + \frac{1}{q_e} \quad (4)$$

Where, q_e and q_t are the amount of adsorbents adsorbed into the adsorbents (mg/g), t is the time (minutes), and k_1 (min^{-1}) and k_2 (g/mg.min) are the constant speeds on the pseudo first and second order.

The constant values determined from the slopes and the intercepts of the plot were given in Table 3 and the pseudo first order and pseudo second order plots were shown in Figure 9A and 9B. The R^2 value for pseudo first order from S-24 (0.990), S-48 (0.841) and S-standard (0.987) are lower in comparison to the R^2 values for pseudo second order, which are 0.99; 0.983; and 0.998 respectively. The R^2 values for pseudo second order kinetic is also approaching one and therefore we suggest that the adsorption of Pb^{2+} onto sodalite surface followed a second order reaction.

3.4.3. Isotherm adsorption

Langmuir's and Freundlich's isotherms models were used to provide insight into the isotherm adsorption type that represents Pb^{2+} adsorption on sodalite surface. Langmuir's isotherm model described monolayer adsorption in homogeneous surfaces without further interaction between the adsorbed molecule and remaining substrates [23]. Langmuir's equation model was calculated based on following derived equation:

$$\frac{C_e}{q_t} = \frac{1}{q_0 K_L} + \frac{C_e}{q_0} \quad (5)$$

Where, K_L is the adsorption equation constant (L.mg^{-1}), q_0 is the maximum adsorption capacity in monolayers, q_e is the amount of adsorbates in each grams being adsorbed into the adsorbent (mg.g^{-1}) in the concentration (Ce) (mg.L^{-1}). The experimental isotherm data was obtained by plotting a line between Ce/qe versus Ce. An important characteristic from Langmuir's equation is stated with dimension separation characteristic (R_L), which is defined below:

$$R_L = \frac{1}{(1 + K_L C_0)} \quad (6)$$

Where, Co is the initial solution concentration (mg.L^{-1}), K_L is Langmuir's adsorption constant (L.mg^{-1}). R_L value shows the suitability of the adsorption, where if ($R_L > 1$) means unsuitable adsorption, if ($R_L = 1$) shows a linear adsorption, if ($0 < R_L < 1$) shows a linear adsorption and if ($R_L > 1$) shows an irreversible adsorption. The Freundlich's isotherm model was also used to determine the parameters that are related to the adsorption characteristics occurs

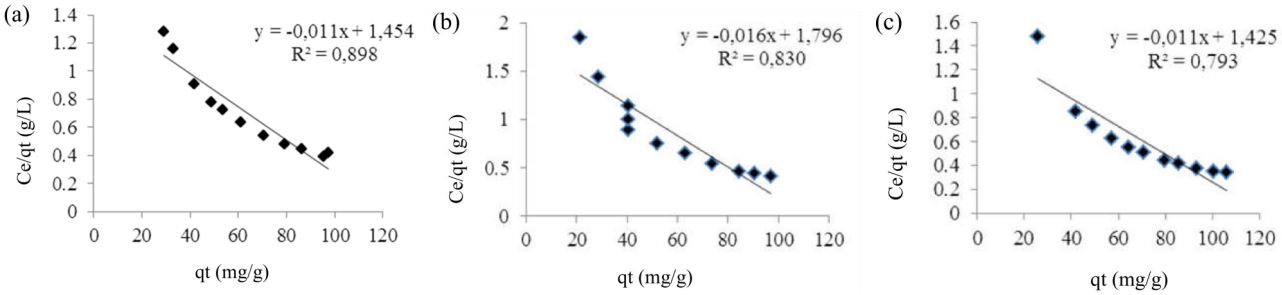

Figure 10. Langmuir's isotherm adsorption model of Pb^{2+} on sodalite, (a) S-24, (b) S- 48,(c) S-standard

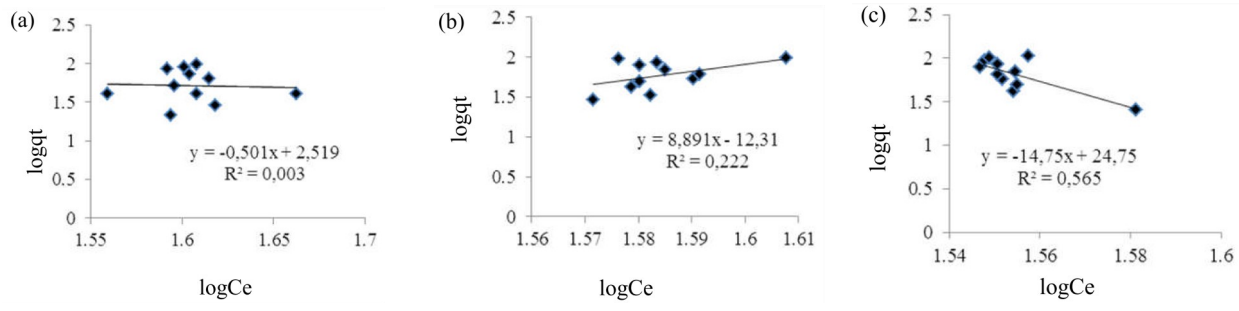

Figure 11. Freundlich isotherm adsorption model of Pb^{2+} on sodalite (a) S-24, (b) S-48, (c) S-standard

Copyright © 2019, BCREC, ISSN 1978-2993

on heterogeneous systems (Equation (7)).

$$ln(q_e) = \frac{1}{n} ln(C_e) + ln\ K_F \quad (7)$$

Where, K_F ((mg.g^{-1})(L.g^{-1})^n), $1/n$ is the Freundlich constant that is related to the adsorption capacity and intensity of the adsorbent. C_e and q_e are the same as explained previously based on Langmuir's isotherm model.

Data derived from Langmuir's isotherm adsorption model and the Freundlich isotherm adsorption model were shown in Table 4 and a linear curve obtained from the plots shown in Figures 10 and 11, respectively. The Freundlich isotherm model, however, has lower R^2 value in comparison to the Langmuir's isotherm model. It is suggested that the adsorption of Pb^{2+} on sodalite surface followed Langmuir's isotherm model which implied that the adsorption occurred mimicking the adsorption on the surface of homogeneous materials through a monolayer adsorption. The Langmuir's isotherm model also suggested that multilayer adsorption involving the adsorbed Pb^{2+} ions on the sodalite surface with Pb^{2+} ions in the solution is impossible under such conditions [24].

4. Conclusion

Synthesis of sodalite from raw kaolin was investigated in detail that revealed the transformation occur via formation of zeolite-A. Sodalite was synthesis by varying of stirring and aging times, Si/Al ratios, and water composition. The as-synthesized sodalite was then used as adsorbent for Pb^{2+} ion for heavy metal treatment. The kinetic studies indicated that the adsorption of Pb^{2+} occurred through monolayer adsorption of Pb^{2+} on the surface without further interactions between the adsorbed molecules with the remaining Pb^{2+}. These limit the sodalite adsorption ability to reach steady state after 250 minutes the reaction. The maximum Pb^{2+} adsorption capacity being adsorbed into sodalite synthesized from kaolin obtained at 24 h and 48 h of crystallization (S-24 and S-48) and sodalite synthesized from commercial silica (S-standard) are 95, 90, and 100 mg/g, respectively.

Acknowledgments

The Authors would like to give credentials to the Ministry of Research, Technology, and Higher Education of Republic of Indonesia, for funding this research through *Penelitian Unggulan Perguruan Tinggi* (PUPT), research grant No. 003246.18/IT2.11/PN.08/2016 and 593/PKS/ITS/2017.

Table 3. Constants derived from the pseudo first and second order models to represent the kinetic of Pb^{2+} adsorption on sodalite

Adsorbent	C_o (mg.L^{-1})	q_e(exp)^a (mg.g^{-1})	Pseudo first order models			Pseudo second order models		
			$q_e{}^a$ (mg.g^{-1})	k_1 (min^{-1})	R^2	$q_e{}^a$ (g.mg^{-1})	k_2 (g.mg^{-1}.min^{-1})	R^2
S-24	50	95.31	68.8548	0.004	0.990	111.11	0.0000978	0.997
S-48	50	90.47	67.6265	0.005	0.841	111.11	0.0000658	0.983
S-standard	50	100	68.3061	0.004	0.987	111.11	0.0000116	0.998

q_e(exp)^a and q_e are experiments and calculated values of q_e.

Table 4. Isotherm parameters of Pb^{2+} adsorption on sodalite derived from Langmuir's isotherm and Freundlich Isotherm models.

Adsorbent	Langmuir's Isotherm				Freundlich Isotherm		
	K_L (L/mg)	q_m (mg/g)	R_L	R^2	K_F (L/mg)	1/n	R^2
S-24	0.0075	90.9	0.7479	0.898	1.09025	0.11247	0.222
S-48	0.0089	62.5	0.7161	0.830	0.40122	1.99601	0.003
S-standard	0.0077	90.9	0.7442	0.793	1.39357	0.06779	0.793

Copyright © 2019, BCREC, ISSN 1978-2993

References

[1] Gupta, V.K., Ali, I. (2004). Removal of Lead and Chromium from Wastewater using Bagasse Fly-Ash-a Sugar Industry Waste. *Journal of Colloidal Interface Science*, 271: 321-328.

[2] Pearce, J.M.S. (2007). Burton's Line in Lead Poisoning. *Europion Neurology*, 57: 118-119.

[3] Barakat, M.A. (2011). New Trends In Removing Heavy Metals From Industrial Wastewater. *Arabian Journal of Chemistry,* 4: 361-377

[4] Kurniawan, T.A., Chan, G.Y.S., Lo, W.Y., Babel, S. (2006). Physicochemical Treatment For Wastewater Laden with Heavy Metal. *Chemical Engineering Journal*, 118: 83-98.

[5] Albanis, T. (2009). *Pollution and Environmental Protection Technologies*. Tzillas Publications, Greek, ISBN 978-960-418-206-0.

[6] Charerntanyarak, L. (1999). Heavy Metals Removal by Chemical Coagulation and Precipitation. *Water Science Technology*, 39(10-11): 135-138.

[7] Mobasherpour, I., Salahi, E., Pazouki, M. (2016). Comparative of The Removal of Pb^{2+}, Cd^{2+}, and Ni^{2+} by Nano Crystallite Hydroxyapatite from Aqueous Solutions : Adsorption Isotherm Study. *Arabian Journal of Chemistry*, 5: 439-446.

[8] Sreejalekshmi, K.G., Krishnan, K.A., Anirudhan, T.S. (2009). Adsorption of Pb(II) and Pb(II)-Citric Acid on Sawdust Activated Carbon. *Journal Hazard Material*, 161: 1506-1513.

[9] Visa, M. (2016). Synthesis and Characterization of New Zeolite Materials Obtained from Fly Ash for Heavy Metals Removal in Advanced Wastewater Treatment. *Powder Technology*, 294: 338-347.

[10] Batabyal, D., Sahu, A., Chaudhuri, S.K. (1995). Kinetics and Mechanism of Removal of 2,4-Dimetyl Phenol from Aqueous Solutions with Coal Fly Ash. *Separation Technology*, 5(4): 179-186.

[11] Petrus, R., Warchol, J.K. (2005). Heavy Metal Removal by Clinoptilolite. An Equilibrium Study Iin Multi-Component System. *Water Resources*, 39: 819-830.

[12] Jiang, J., Gu, X., Feng, L., Duanmu, C., Jin, Y., Hu, T., Wu, J. (2012). Controllable of Sodalite Submicron Crystal and Microspheres from Palygorskite Clay Using a Two-Step Approach. *Powder Technology*, 217: 298-303.

[13] Naskar, M.K., Kundu, D., Chatterjee, M. (2011). Coral-like Hydroxyl Sodalite Particle from Rice Husk Ash as Silica Source. *Material Letters*, 65: 3408-3410.

[14] Yu, H., Shen, J., Li, J., Sun, X., Han, W., Liu, X., Wang, L. (2014). Preparation, Characterization and Adsorption Properties of Sodalite. *Material Letters*, 132: 259-262.

[15] Ghazemi, Z., Younesi, H., Kazemian, H. (2011). Synthesis of Nano Zeolite Sodalitefrom Rice Husk Ash without Organic Additives. *Canadian Journal of Chemical Engineering*, 89: 601-608.

[16] Prokof'ev, V. Yu., Gordina, N.E. (2014). Preparation of Granulated and SOD Zeolites from Mechanically Activated Mixtures of Metakaolin and Sodium Hydroxide. *Applied Clay Sciences*, 101: 44-51.

[17] Qoniah, I., Prasetyoko, D., Bahruji, H., Triwahyono, S., Jalil, A.A., Suprapto, S., Hartati, H., Purbaningtias, T.E. (2015). Direct Synthesis of Mesoporous Aluminosilicates from Indonesian Kaolin Clay without Calcination. *Applied Clay Sciences*, 118: 290-294.

[18] Alkan, M., Hopa, C., Yilmaz, Z., Güler, H. (2005). The Effect of Alkali Concentration and Solid/Liquid Ratio on The Hydrothermal of Zeolite NaA from Natural Kaolinite. *Microporous Mesoporous Material*, 86: 176-184.

[19] Hiyoshi, N., (2012). Nanocrystalline sodalite: Preparation and Application of 2-Cyclohexen-1-One with Hydrogen Peroxide, *Applied Catalysis A: General*, 419-420: 164-169.

[20] Zhang, X., Tong, D., Jia, W., Tang, D., Li, X., Yang, R. (2014). Studies on Room-Temperature of Zeolite NaA. *Materials Research Bulletin,* 52: 96-102.

[21] Wang, J-Q., Huang, Y-X., Pan, Y., Mi, J-X. (2014). Hydrothermal of High Purity Zeolite A from Natural Kaolin without Calcinations. *Microporous Mesoporous Material*,199: 50-56.

[22] Li, Q., Mihailova, B., Creaser, D., Sterte, J. (2001). Aging Effect on The Nucleation and Crystallization Kinetics of Colloidal TPA-silicate-1. *Microporous Mesoporous Material*, 43: 51-59.

[23] Zhang, M.L., Zhang, H.Y., Xu, D., Han, L., Niu, D.X., Tian, B.H., Zhang, J., Zhang, Y., Wu, W.S. (2011). Removal of Ammonium from Aqueos Solutions using Zeolite Synthesized from Fly Ash by A Fusion Method. *Desalination,* 271: 111-121.

[24] Kocaoba, S., Orhan, Y., Akyuz, T. (2007). Kinetics and Equilibrium Studies of Heavy Metal Ions Removal by Use of Natural Zeolite. *Desalination*, 214: 1-10.

[25] Rayalu, S.S., Udhoji, J.S., Meshram, S.U., Naidu, R.R., Devota, S. (2005). Estimation of Crystallinity in Fly ash-based Zeolite-A using XRD and IR Spectroscopy. *Current Science*, 89(12): 2147–2151.

Copyright © 2019, BCREC, ISSN 1978-2993